Chapter 4
Tunneling in Electron Transport

Christopher C. Moser

Abstract Light excitation of chlorophylls and bacteriochlorophylls creates strong reductants to initiate guided electron transfer through chains of redox centers, converting light energy into electrostatic and chemical redox energy and largely avoiding the threat of charge recombination unless useful. Most electron-transfer reactions of photosynthesis are single-electron transfers between well-separated redox centers via electron tunneling through the insulating intervening protein medium. Tunneling rates are dominated by an exponential dependence on the edge-to-edge distance between cofactors. There is an approximately Gaussian dependence of rate on driving force, with a peak rate at the reorganization energy, as defined by classical Marcus theory and modified to include quantum effects. Complex quantum theoretical rate dependencies are well approximated by a simple empirical expression with three parameters: distance, driving force, and reorganization energy. Natural selection exploits distance and driving force to speed desirable electron transfers or slow undesirable electron transfer. Redox centers engaged in productive electron transfer are placed less than 14 Å apart. Natural photosynthetic proteins are far from ideal: they have high yields but a superabundance of cofactors and relatively large energy losses.

Keywords Electron-transfer chains • Electron tunneling • Marcus theory • Photosynthesis • Reaction centers • Reorganization energy

C.C. Moser, Ph.D. (✉)
Department of Biochemistry and Biophysics, University of Pennsylvania,
422 Curie Blvd, Philadelphia, PA 19104-6059, USA
e-mail: moserc@mail.med.upenn.edu

J. Golbeck and A. van der Est (eds.), *The Biophysics of Photosynthesis*,
Biophysics for the Life Sciences 11, DOI 10.1007/978-1-4939-1148-6_4,

Abbreviations

ADP	Adenosine diphosphate
ATP	Adenosine triphosphate
NADH	Reduced nicotinamide adenine dinucleotide
PSI	Photosystem I
PSII	Photosystem II
λ	Reorganization energy
ΔG	Free energy of reaction
$\hbar\omega$	Characteristic frequency of vibration coupled to electron transfer

4.1 Concept 1: Light Excitation of Chlorophylls and Bacteriochlorophylls Creates Strong Reductants for Charge Separation

The act of exciting a photosynthetic pigment promotes an electron to a higher energy level and leaves an empty orbital behind. This simultaneously creates a good reductant in the excited electron, and a good oxidant in the empty orbital or "hole" left behind. While the light-activated flavoproteins such as photolyase or cryptochrome [1, 2] use the excited state as a photo-oxidant, filling the emptied orbital with an electron from a nearby reductant such as tryptophan or tyrosine, the chlorophylls and bacteriochlorophylls of photosynthesis are biased to act as photo-reductants such that the initial electron transfer is the reduction of a nearby redox cofactor by the excited pigment.

The chlorins and bacteriochlorins of photosynthesis are tetrapyrrole rings with extensive conjugation of two dozen nitrogen and carbon p-orbitals that leads to large molecular orbitals about 10 Å across. This means that light absorption will be red-shifted from the typical ultraviolet absorption of smaller organic molecules into the red and infrared regions, respectively. The lowest excited-state energies associated with these electronic transitions are around 1.8–1.1 eV (deep red 680 nm to infrared 1,100 nm). With an oxidation/reduction potential of the ground-state chlorophyll of +1.26 (vs. the standard hydrogen electrode) in PSII [3], the absorbed photon lowers the reducing potential of the excited singlet state to ~ −0.57 V. The protein environment of the P700 chlorophyll of PSI lends the ground-state pigment considerably more reducing power at ~0.45 V [4]; even though the absorbed photon has nearly the same energy, the excited singlet state is also much more reducing, ~−1.32 V. These excited state redox potentials are low enough to reduce most biological redox centers.

4.2 Concept 2: Photosynthesis Uses Light-Activated Charge Separation and Guided Electron Transfer to Convert Light Energy into Electrostatic and Chemical Redox Energy

In natural photosynthetic proteins, redox centers are placed relatively close together so that electrons are guided by proximity through a series of redox cofactors assembled across a bioenergetic membrane (Fig. 4.1) that are, to first approximation, progressively more oxidizing. This results in the loss of reducing power, but converts the electrostatic energy of charge separation into a transmembrane electric field. When the electron reaches a quinone redox center in PSII and purple sulfur bacterial reaction centers, reduction may be accompanied by the uptake of a proton, contributing to transmembrane proton gradients. The transmembrane electric field and proton gradient represent an electrochemical proton gradient. This distributed energy currency can be used to power other transmembrane events such as the pumping of molecules across the membrane counter to their concentration gradients or into the energetically uphill chemical reaction of phosphorylating ADP to ATP using the transmembrane ATPase protein. The redox energy of the original charge separation is preserved in relatively stable form in chemical oxidants and reductants. In the case of plant photosynthesis, this is molecular oxygen, the product of water splitting in PSII, and chemically reduced species such as NADH or glucose.

4.3 Concept 3: Charge Recombination Poses the Threat of Energy Loss, Though Sometimes This Is Useful

The progressive charge separation along the chain of redox cofactors competes with charge recombination to either an excited state or the low-energy ground state. Electron spins are important in the both the time scale and energetics of charge recombination. At first, the light-excited electron maintains the same spin state as in the ground state; both are called singlets. Charge recombination to the excited state can occur before electron spins rephase, recreating the excited singlet state, which can again engage in productive electron transfer or return to the ground state by emitting a photon in fluorescence. Alternatively, charge recombination can short-circuit to the ground state, which has the net effect of turning light energy into heat. Normal fluorescence of chlorins and bacteriochlorins occurs on the nanosecond time scale [8]. Emission from this thermally assisted return of the electron to the singlet state is called delayed fluorescence. During the time of charge separation, magnetic interactions can rephase the electron spin from singlet to triplet; in this case charge recombination occurs to a generally lower energy-excited triplet state. As the spins must flip to recreate the singlet ground state, return to the ground state is considerably slower,

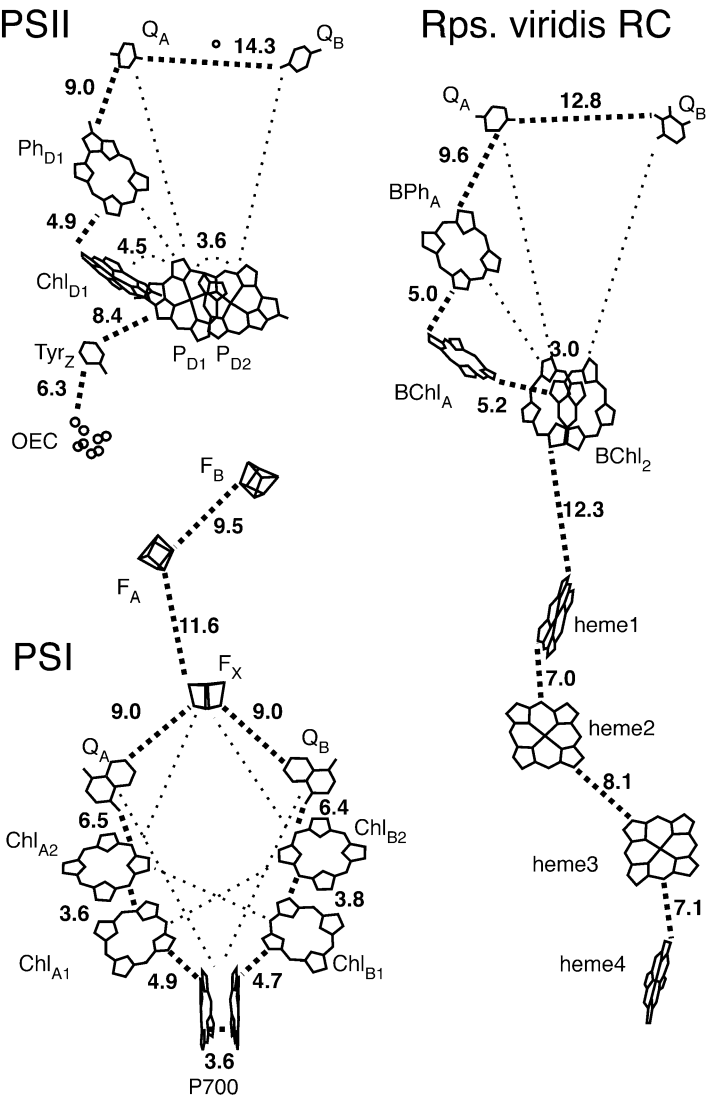

Fig. 4.1 Productive electron transfer is guided across the membrane (vertical direction) in natural photosynthetic reaction centers by the proximity of the redox cofactors. Productive reactions are *thick dashed lines*, unproductive short circuits are *thin*. Photosystem I and II use chlorophylls ChlD1 and P700 as light-activated centers and the photosynthetic bacteria use a bacteriochlorophyll $BChl_2$. Edge-to-edge distances between cofactors are given by crystal structures available in the PDB database 1JBO [5], 1S5L [6], and 1PRC [7]

emitting a lower energy photon in phosphorescence. Magnetic sensitivity allows flavoproteins in some organisms to sense the earth's magnetic field direction.

Although loss of the light energy in the form of lower energy photons and heat due to charge recombination is not bioenergetically productive, it can nevertheless

have important survival value. Under high-light conditions, or when assembly of the photosystems are incomplete, charges can be separated faster than they can be consumed by the rest of the photosynthetic machinery. The powerful oxidizing and reducing radicals created by light excitation can create unintended and destructive side reactions, compromising the protein structure or the pigment and redox cofactors themselves. Triplet states can also react with triplet molecular oxygen to create singlet oxygen, which is aggressively chemically reactive and can destroy nearby pigments [9]. The half-life of singlet oxygen is only about 200 ns in cells [10] allowing reactions within 10 nm of the site of production [11]. Indeed, the central subunit of PSII is replaced with regularity during normal operating conditions, presumably because of just such destructive reactions [12].

4.4 Concept 4: Most Electron-Transfer Reactions of Photosynthesis Are Single-Electron Transfers Between Well-Separated Redox Centers via Electron Tunneling Through the Insulating Intervening Protein Medium

Only a minority of electron transfers in photosynthesis occur by direct contact between diffusing oxidants and reductants. One such example is the collisional interaction between reduced NADH and oxidized flavin that can transfer a two-electron-carrying hydride group from the nicotinamide to the flavin. In the majority of electron-transfer reactions, rather than group transfer of pairs of electrons, electrons are delivered one at a time from reductants to oxidants [13, 14]. Single-electron transfer is the general rule even in cases of coupled two-electron-transfer reactions, where the second following electron transfer may be so much faster than the first that the single-electron-transfer intermediate cannot be separately observed [13]. Because the amino acids and occasional water molecules that make up the protein medium are relatively difficult to oxidize or reduce, protein acts as an electrical insulator. The single-electron transfers between redox centers that are not in direct contact must traverse the electrically insulating gap between redox centers by electron tunneling [15].

According to classical physics, the electron does not have the energy to exist in the medium between donor and acceptor, far from the donor. But quantum physics describes the electron as a wave function that can extend into this barrier region. That tunneling was indeed a central part of biology was first clearly demonstrated in photosynthetic systems, as revealed by the temperature independence of electron-transfer rates at cryogenic temperatures in photosynthetic reaction centers [16]. This temperature independence at low temperatures eliminates the possibility that some sort of thermally activated classical reaction might be taking place.

4.5 Concept 5: Electron-Tunneling Rates Are Dominated by an Exponential Dependence on the Distance Between Cofactors

Electron tunneling between well-separated redox centers in proteins is dependent upon the extent of overlap of the relevant orbitals for the electron in the donor and the acceptor—the better the overlap, the faster the rate. The wave functions tail off approximately exponentially with the distance between the cofactors, with the result that the maximum electron-tunneling rate trends to a steep exponential decay with edge-to-edge distance between cofactors (Fig. 4.2). In proteins, this coefficient of exponential decay is around 1.4 $Å^{-1}$ on a natural log scale or 0.6 $Å^{-1}$ on a common log scale [17]. This means that the electron tunneling will be ten times slower for every 1.7 Å added to the donor-to-acceptor edge-to-edge distance. The maximal electron-tunneling rate is around 10^{13} s^{-1} at distances approaching van der Waals contact, which is essentially the same as the pre-exponential term k_BT/h in Eyring's 1935 absolute reaction rate theory [18, 19], in which k_B is Boltzmann's constant, T absolute temperature, and h Planck's constant. The protein medium acts as a condensed phase that propagates wave functions better than a vacuum but not as well as a direct covalent link between redox cofactors [17].

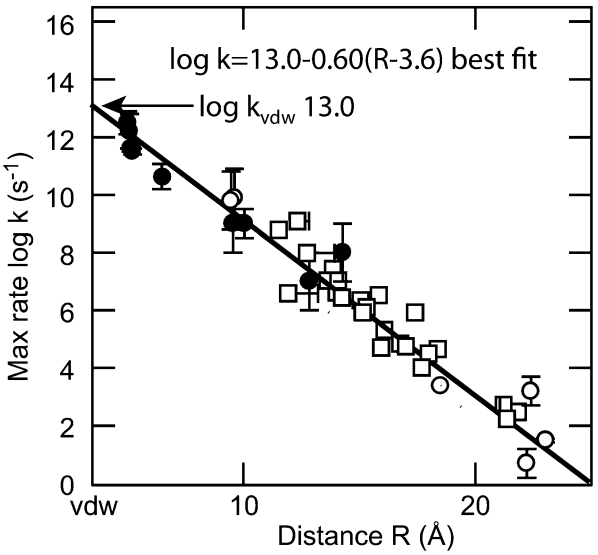

Fig. 4.2 Free energy-optimized rates of electron tunneling in proteins show an exponential dependence with edge-to-edge distance between cofactors [20]. Productive and unproductive electron transfers in photosynthetic reaction centers shown as *filled* and *open circles*, respectively [17]. *Open squares* represent electron transfers in non-photosynthetic and modified protein systems

4.6 Concept 6: Reorganization Energy Dictates the Driving Force Dependence of Electron-Tunneling Rates

Although electron tunneling is an essentially quantum mechanical phenomenon, in order for an electron to tunnel from one center to another, the donor and acceptor orbitals must be at least temporarily at equal energies, even if the overall electron-transfer reaction is energetically favorable and the equilibrium energy of the electron on the donor will be greater than the equilibrium energy on the acceptor. As the atomic nuclei fluctuate in thermal motion, the relative energies of the electron on the donor and acceptor will change for certain atomic motions that are said to be "coupled" to electron transfer. In the 1950s Marcus applied a classical harmonic oscillator viewpoint to these motions [21]. Simple harmonic oscillators have a parabolic dependence of their energy as the nuclei vibrate on either side of an equilibrium, low-energy geometry. The generalized energy surface of the reactant donor/acceptor pair with the electron on the donor is shown as the thick curve in Fig. 4.3. A similar surface applies to the energy of the product donor/acceptor pair (thin curves), with the electron now on the acceptor, but with a different equilibrium nuclear geometry and free energy at the bottom of the product parabola.

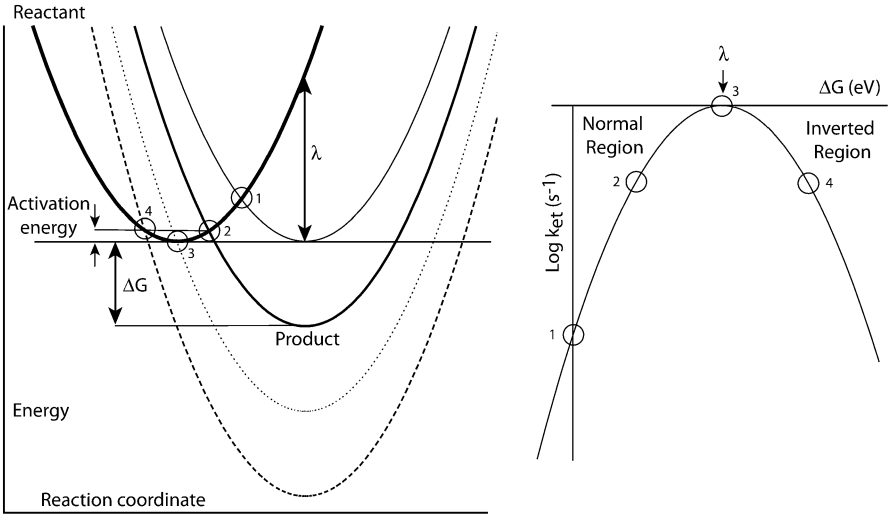

Fig. 4.3 Marcus theory considers the intersection of the energy surfaces of classical simple harmonic oscillators (*parabolas*) along a generalized reaction coordinate (*left*). The intersection of the reactant (with the tunneling electron on the donor) with the product (electron on the acceptor) takes place at different activation energies depending on the driving force for electron transfer ($-\Delta G$). Four different ΔG values are shown (1–4), all with the same reorganization energy (λ); for convenience only one ΔG and one activation energy are labeled that associated with product energy surface 2. On a log rate scale (*right*), this gives a parabolic dependence of rate on driving force with "normal" and "inverted" regions where increased driving force speeds or slows the reaction, respectively

For simplicity, we assume that there is a roughly similar frequency for the vibrational wells of the reactants and products, differing mainly in nuclear and energetic displacement. If we follow the thick energy curve of the reactant to the right as its nuclei are vibrationally moved to resemble the equilibrium geometry of the reactant, but without allowing the electron to be transferred, we would need to add energy lambda, called the reorganization energy.

This reorganization energy λ can be combined with the overall driving force for the electron transfer, $-\Delta G$, to give a classical activation energy for the electron-transfer reaction, that is, the amount of thermal energy that must be added to the equilibrium reactants in order to reach the intersection of the reactant and product surfaces: $E^{\ddagger} = (\Delta G + \lambda)^2/4\lambda$. These intersections are circled and numbered in Fig. 4.3. The activation energy for an electron transfer will begin at λ/4 when there is no net driving force for the reaction (thin curve in Fig. 4.3), and decrease to zero, for an activationless electron transfer, when the driving force matches the reorganization energy (dotted curve). In other words, the reactant ground state is the transition state. All other factors, such as the edge-to-edge distance between donor and acceptor, being the same, this will be the maximal rate at which the electron transfer can occur. If the driving force for electron transfer is even greater than the reorganization energy (dashed curve), then the activation energy will begin to rise again. Counterintuitively, Marcus theory predicts that providing more driving force for a reaction can actually slow the reaction rate. This situation in which the driving force is greater than the reorganization energy is called the Marcus inverted region, and has important significance for the design of photosynthetic systems.

The driving force and reorganization energy dependence of the electron-tunneling rate according to classical Marcus theory is as follows:

$$\text{ket} \propto \frac{1}{\sqrt{4\pi\lambda k_B T}} e^{-(\Delta G+\lambda)^2/4\lambda k_B T} \tag{4.1}$$

Classical Marcus theory predicts a Gaussian dependence of the electron-transfer rate as a function of the driving force with a peak value at λ. This Gaussian curve appears parabolic on a log rate scale (Fig. 4.4). Typical reorganization energies for biological electron-transfer reactions are around 0.7–1 eV. Larger reorganization energies, up to about 1.4 eV, are found for systems in relatively polarizable or mobile polar environments (often near protein surfaces) and with smaller cofactors for donors and acceptors. Under these conditions the change in the distribution of electric charge on moving from donor to acceptor will be more concentrated, which generally leads to a larger reorganization of the electric dipoles in the cofactor environments. Conversely, smaller reorganization energies are associated with larger cofactors and relatively immobile and low dielectric environments (often deeply buried), as the charge changes are more diffuse and the protein environment around the cofactors is less subject to reorganization on electron transfer. The most reliable way to experimentally estimate the reorganization energy of any protein

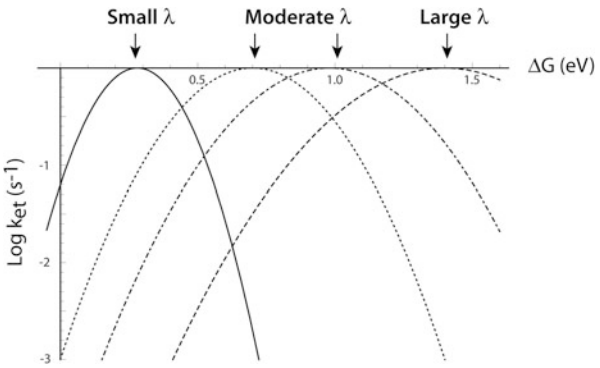

Fig. 4.4 The classical Marcus theory model for the free energy dependence of electron tunneling on driving force is parabolic on a log rate scale with a maximum when the driving force matches the reorganization energy (λ). The reorganization energies shown cover the typical biological range. A comparison can be made with Fig. 4.3: smaller reorganization or larger reorganization energies would correspond movement of the product parabola to the *left* or the *right* (smaller or larger change in nuclear coordinates) in that figure

electron-tunneling reaction is to make progressive changes in the driving force by chemical substitution of the donor or the acceptor and look for a Marcus-like dependence. This has been done for a number of different photosynthetic electron-transfer reactions [22–26].

4.7 Concept 7: The Initial Charge Separation of Photosynthesis Exploits the Marcus Inverted Region to Make Charge Recombination Slower than Charge Separation

After light excitation of a photosynthetic reaction center pigment and the initial reduction of the nearby acceptor molecule, there is a competition between electron transfer to another acceptor to further separate charges and charge recombination to the ground state. With a modest, energy-conserving driving force for the initial electron transfer compared to the exciting photon energy, the driving force for the charge recombination to the ground state is large. When the reorganization energy for the electron transfer between the excited pigment and the acceptor is less than half the photon energy, then the initial electron transfer will be in the "normal" Marcus region and the charge recombination in the "inverted" region (Fig. 4.5). This has the effect of slowing down the charge recombination by many orders of magnitude and allows time for a second, productive electron transfer to take place further separating charges. Without exploiting the Marcus inverted region, is it difficult to construct light-activated charge-separating systems that have both high

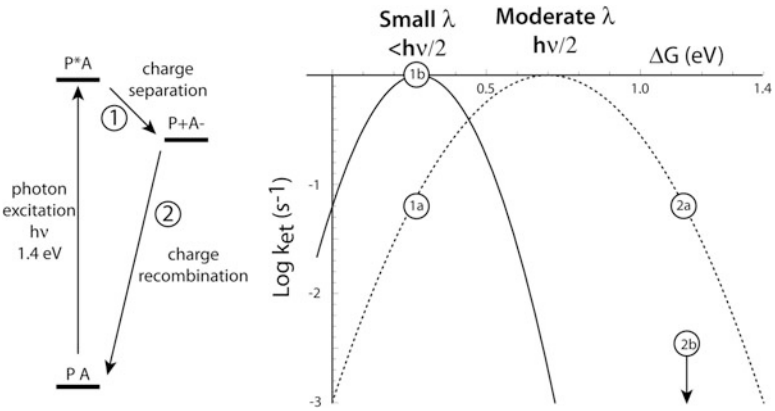

Fig. 4.5 For light-activated charge separations, the productive initial charge separation (*left*) competes with the loss reaction of charge recombination to ground state over the same distance. If the reorganization energy is half the energy of the excited state, both these electron-transfer steps will have the same rate (*1a* and *2a* at *right*) and the net loss can be high. If the reorganization energy is less than half the excited state energy, then the charge separation will be slower than the charge recombination (*1b* and *2b*), because the former is in the normal region, and the latter in the inverted region

quantum efficiency of charge separation and good conservation of the photon energy in the form of the redox energy difference between product oxidants and reductants. This can be seen in a survey of the present generation of synthetic photochemical dyads and triads.

4.8 Concept 8: For Biological Cofactors, Classical Marcus Theory Needs to Be Modified to Include Quantum Effects on the Driving Force Dependence

While classical Marcus theory is roughly applicable to biological electron-transfer systems, a closer look at the temperature dependence of those systems in which the driving force has been systematically changed by altering the redox properties of the donors and acceptors shows that the classical approach must be modified to include quantum terms not only for the tunneling electron but also for the vibrating nuclei.

The most obvious demonstration of this effect is seen when photosynthetic reactions are followed at cryogenic temperatures. The classical Marcus theory predicts an increasingly sharp falloff of the rate as the driving force departs from the optimum at $-\Delta G = \lambda$ as the temperature is lowered (Fig. 4.6). Essentially, lower temperatures make it harder to thermally surmount the Marcus activation energy barrier and only nearly activationless reactions can proceed at the lowest temperatures.

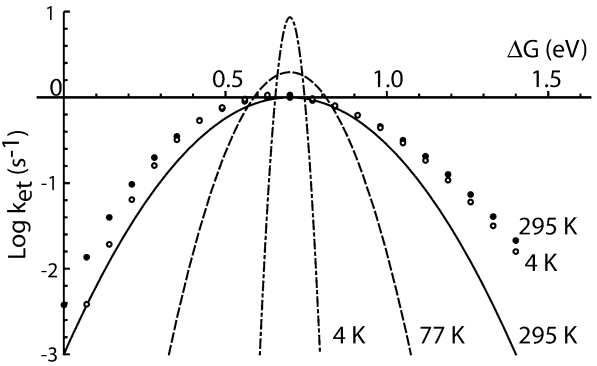

Fig. 4.6 The temperature modulation of classical Marcus (*lines*) and quantum single (*dots*) harmonic oscillator models of the driving force dependence of electron-tunneling rates. The lack of strong temperature dependency for many biological electron transfers indicates that relatively high-energy quantum nuclear vibrations are coupled to electron transfer

As seen in the original DeVault and Chance experiments [16] and in the extensive quinone substitution experiments of Gunner et al. [22, 25], the Marcus curve sharpening fails to materialize at cryogenic temperatures. It is clear that there are vibrations that are coupled to electron transfer that are comparable to or greater than the Boltzmann thermal energy k_BT at room temperature, and that these high-energy vibrations must be treated in a quantum tunneling rather than classical manner. These same experiments show that the driving force dependence of the rate, even at room temperature, is noticeably broader than that implied by the classical Marcus treatment.

There are several approaches to introducing the quantum effects of relatively large energy vibrations to electron tunneling in proteins [15]. Hopfield [27] presents a mathematically simple, semiclassical method which uses a trigonometric Coth term that reverts to the Marcus classical expression at high temperatures, but merges into a temperature-independent form at thermal energies below the characteristic quantum frequency of vibration coupled to the electron transfer, $\hbar\omega$:

$$ket \propto \frac{1}{\sqrt{2\pi\lambda\hbar\omega \mathrm{Coth}[\hbar\omega/2k_BT]}} e^{-(\Delta G+\lambda)^2/2\lambda\omega \mathrm{Coth}[\hbar\omega/2k_BT]} \tag{4.2}$$

The Hopfield expression maintains the Marcus simplicity of a Gaussian dependence of rate on driving force, but yields a broader Gaussian when vibrational modes larger than room temperature k_BT are coupled to electron transfer.

A fully quantum treatment of an electron transfer coupled to a quantized simple harmonic oscillator of energy $\hbar\omega$ requires a modified Bessel function [28]. This is a discrete function that is only defined at energy intervals of $\hbar\omega$, corresponding to

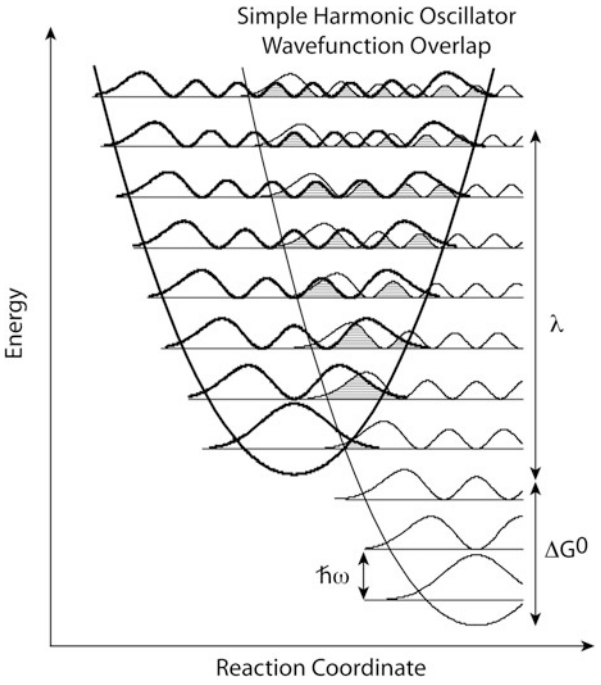

Fig. 4.7 To capture the nuclear dependent terms in electron tunneling, a simple quantum harmonic oscillator picture describes the overlap (hatching) of reactant and product wave functions (approximated here as the square of the wave functions in *wavy lines*) at various energy levels separated by the quantum of vibrational energy $\hbar\omega$

the overlap of vibrational wave functions shown in Fig. 4.7, because only at these ΔG values can the reactant and product be at the same energy at the same nuclear coordinates. An example of this function is plotted in Fig. 4.7 as the separate points:

$$\text{ket} \propto \exp[-(\lambda/\hbar\omega)(2n_k+1)]\left(\frac{(n_k+1)}{n_k}\right)^{\Delta G/2\hbar\omega} I_{\Delta G/\hbar\omega}\left[2(\lambda/\hbar\omega)\sqrt{n_k(n_k+1)}\right] \tag{4.3a}$$

where

$$n_k = 1/\left(\exp[k_B\hbar\omega]-1\right] \tag{4.3b}$$

Practically, electron transfer in proteins takes place smoothly at all driving forces, combining harder high-energy and softer low-energy vibrations to equalize donor and acceptor energies for electron tunneling. The quantum expression of Eq. (4.4) sums all these wave function overlaps. In this equation, S_k is the reorganization energy of the hard vibration in units of $\hbar\omega$; m is the change in the quantum number of the vibration; n_k is the same as in Eq. (4.3b), an expression of the temperature-dependent population of higher vibrational levels; and λ_s

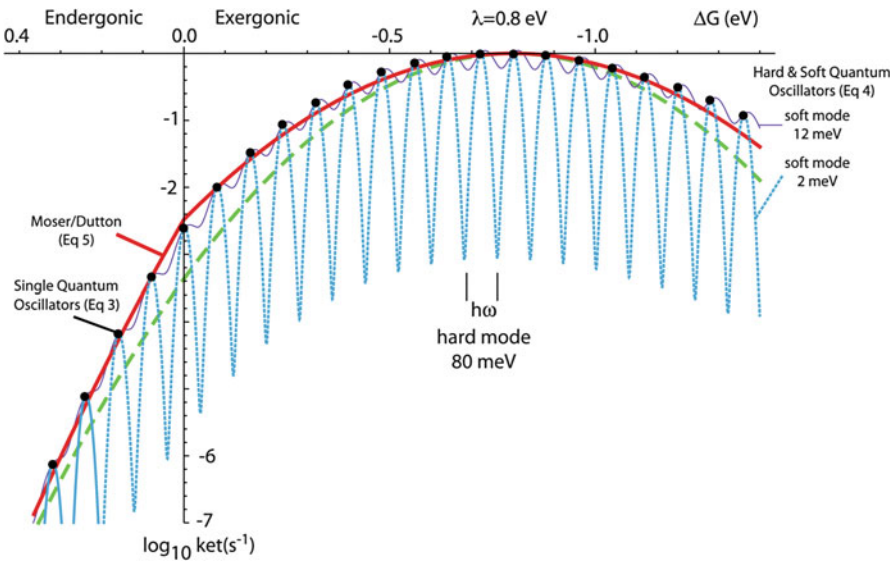

Fig. 4.8 Examples of classical and quantum approaches to the driving force dependence of the rate of electron tunneling. *Dashed line*: The classical Marcus expression at room temperature with a reorganization energy of 0.7 eV. *Black dots*: A single quantized harmonic oscillator with characteristic frequency of 80 meV; in this extreme view the reaction will only occur when ΔG is an integer multiple of this vibration and so is undefined at other ΔG values, defined only at quantized energies. *Dotted line*: Coupled quantized hard (80 meV) and soft (2 meV) energy harmonic oscillators for a continuous curve. *Thin solid line*: Same but with a 12 meV soft mode. *Thick solid line*: The Moser-Dutton simple approximation to quantized harmonic oscillators dominated by a hard vibration

the reorganization energy associated with the soft vibrational modes. Examples of this function are shown as the wavy curves in Fig. 4.8:

$$\text{ket} \propto \frac{\exp[-S_k(2n_k+1)]}{\sqrt{4\pi\lambda_s k_B T}} \sum_{m=-\infty}^{+\infty} \left(\frac{(n_k+1)}{n_k}\right)^{m/2} I_m\left[2S_k\sqrt{n_k(n_k+1)}\right] \exp\left[-\frac{(\lambda_s + m\hbar\omega_k - \Delta E)^2}{4\lambda_s k_B T}\right] \tag{4.4}$$

4.9 Concept 9: The Quantum Dependence on Driving Force Can Be Approximated by a Simple Empirical Expression

The more complex exact quantum expressions are calculation overkill for matching any practical experimental system of electron tunneling in protein. The experimental measurements and parameters are just not precise enough. While appropriate

distances can be reasonably estimated from X-ray crystal structures, driving forces are often poorly known and have significant uncertainties when estimated from equilibrium redox potentials. Reorganization energies are even more uncertain and there is no clear way to measure the characteristic vibrational frequencies coupled to electron transfer, leaving it to be a fit parameter. Furthermore, biological electron-transfer rates themselves are often not well fit by a single exponential time course, but cover a range of rates.

A simple empirical expression [17] that successfully estimates protein electron-tunneling rates with less than an order of magnitude of uncertainty and comparable to experimental errors combines the observed exponential falloff of rate with distance of Fig. 4.1 with a room-temperature version of the Hopfield expression for an exergonic electron-transfer reaction that uses just the three most important parameters:

$$\log k_{et}^{exer} = 15 - 0.6(R - 3.6) - 3.1(\Delta G + \lambda)^2/\lambda \tag{4.5a}$$

where R is the edge-to-edge distance between redox cofactors in Å, ΔG is the free energy of electron transfer, and λ is the reorganization energy, both in units of eV. For the corresponding endergonic electron transfer of the reverse reaction, we use a Boltzmann ratio of rates:

$$\log k_{et}^{ender} = \log k_{et}^{exer} - \Delta G/.06. \tag{4.5b}$$

While the fusion of Eqs. (4.5a) and (4.5b) introduces an esthetically distracting inflection point at zero driving force, we can see from Fig. 4.8 that it presents a remarkably good approximation, well within experimental error, of the much more complex discrete fully quantum simple harmonic oscillator equation, without any of the driving force oscillations that are part of the even more complex quantum high and low vibrational energy model. There is no clear evidence for this type of oscillation in the biological experimental literature. Contrary to some reports [29], there is no inconsistency or mathematical error that arises from using these coupled equations exclusively for the exergonic domain on one hand, and the endergonic domain on the other as an approximation to more unwieldy quantum mathematical expressions. Obviously, it is inappropriate to use the endergonic expression for an exergonic reaction, and vice versa. Equations (4.5a) and (4.5b) are enough to understand the basic engineering and operation of natural electron-transfer proteins and to provide a reliable rule of thumb when modifying natural proteins or designing artificial electron-transfer proteins.

Indeed, with edge-to-edge distances provided by a protein structure and a rough idea of the redox potentials of the redox cofactors and hence the driving force for electron transfer, using this expression with a generic reorganization energies of around 0.9 eV estimates the rate of all the electron-tunneling reactions with an accuracy of about an order of magnitude, enough to understand how the intraprotein

electron-transfer network operates. Or, if there is no structure but intraprotein electron-transfer rates and redox potentials of cofactors are known, then it is possible to predict the distances between redox centers and gain a fair idea of the structure of the protein.

4.10 Concept 10: Natural Selection Has Used Distance and Driving Force to Speed Desirable Electron Transfers or Slow Undesirable Electron Transfer, Not Modification of the Intervening Protein Medium

The distance that an electron can tunnel through a surrounding medium depends on the height of the energetic barrier the electron must tunnel through. The lower the barrier, the faster the electron tunneling for any given distance. It has been shown in many chemical synthetic systems that a direct covalent link between donor and acceptor speeds the electron-transfer rate compared to donors and acceptors separated by solvent [17]. The presence of a dense array of atomic orbitals connecting the donor and acceptor effectively lowers the barrier the electron must tunnel through. In principle, nature could have selected the amino acid structure making the protein medium between a donor and acceptor to resemble a more covalent, bridge-like connection in order to speed useful electron transfers, or to resemble more solvent like or even vacuum like to slow short-circuiting or unproductive electron transfers. The free energy-optimized electron-tunneling rates of Fig. 4.1, representing a collection of both productive charge-separating reactions of photosynthesis and unproductive charge recombinations, as well as a collection of unphysiological rates achieved by introducing extraneous redox centers to natural proteins, show that this is not the case [30].

Natural selection appears to have favored using distance and driving force as the principle means to direct electron transfers in productive directions and avoid unproductive directions. This is likely due to the profound effect that even small changes in distance can have on electron-transfer rates, speeding or slowing by a 100-fold with just a 3.3 Å change in distance. Typically, natural protein scaffolds fix redox centers with relatively little wiggle although, in rare cases, large conformational changes in the protein effectively move redox centers into and out of electron transfer distance. It is apparently much more difficult for natural selection to secure structural changes in the effective tunneling barrier between redox centers over a sufficient distance to achieve a comparable effect on the rate. Instead, donors and acceptors in productive reactions are closer than in unproductive reactions.

Changes in driving force, through mutational changes in redox midpoint potentials, can also be effective in slowing unproductive reactions. All else being equal, a near-zero driving force electron-tunneling reaction is slowed a 100-fold by lowering the redox midpoint of the acceptor by 0.12 V. Much smaller changes will be seen if the driving force more nearly matches the reorganization energy, as is the case for several productive electron transfers in photosynthetic reaction centers.

4.11 Concept 11: Nature Guides the Path of Electron Transfer Mainly Through Placing Redox Centers Close Together, Less than 14 Å

A survey of structures of natural electron-transfer proteins shows conspicuous chains of redox centers, with nearly all redox partners separated by 4–14 Å [31]. This assures that electron-tunneling rates for low-driving-force reactions with typical reorganization energies are in the range of 0.3 ns to 0.3 ms. What this means is that electron tunneling is generally fast enough to not limit the enzymatic turnover of electron-transfer proteins, which are typically in the range of 10^3 s^{-1}, a rate that seems to be limited by protein and substrate diffusion as well as proton transfers that are common in catalysis. There seems to be no pressure for natural selection to achieve faster electron-tunneling rates when the overall performance of catalytic turnover in an electron-transfer system will be unchanged. A corollary of this observation is that if two redox centers in a protein are separated by more than 14 Å, then they are likely not natural redox partners.

While distances towards the long end of this range may be acceptable for most electron transfers of respiration and photosynthesis, the initial light-induced charge separation reactions compete with the usually unproductive decay of the excited state of the ns time scale. Natural selection has favored initial charge separations at the short end of this distance scale and fast enough to assure a high quantum yield of charge separation.

4.12 Concept 12: Natural Photochemical Systems Are Not Ideal. They Have High Yields, but a Superabundance of Cofactors and Relatively Large Energy Losses

In spite of a common belief that many millions of years of natural selection must have created protein systems in which each component has been optimized and that natural designs are near perfect and cannot be improved, photosynthetic systems are not perfect but simply good enough to work in a biological context. In many ways natural photosystems are a poor model for molecular designers to mimic while attempting to create artificial systems to harvest sunlight. Using the empirical electron-tunneling expressions (4.5a) and (4.5b) it is a simple matter to demonstrate that photochemical triads embedded in protein, with donor, light-activated pigment and acceptor in an approximately linear arrangement, can preserve significantly more of the energy of the absorbed photon in the redox difference between the photo-oxidized donor and photo-reduced acceptor, at any selected time scale, than is seen in any natural photosystem. For example, such a triad could have greater than 80 % efficiency on a millisecond time scale, while natural photosystems operate at closer to 50 % energetic efficiency.

Lowered overall energetic efficiency presumably reflects the evolution of natural photosystems in a bioenergetic legacy that could make little use of more energetically efficient designs. For example, reliance on membrane-diffusible quinones with redox midpoint potentials around 0 mV to connect photosynthetic protein modules means that there is no effective way to preserve the low redox potential of the highly reducing light-activatable donors in purple bacterial reaction centers or PSII. Instead these systems have much larger driving force drops between cofactors than are needed to achieve rapid enough charge separation through electron tunneling to avoid unproductive charge recombination reactions. More than half the energy of the photon is lost as heat. It is true that the quantum efficiency of natural photosystems is high, approaching 100 %, but this comes along with significant loss of redox energy that could otherwise be harnessed in designed artificial systems.

PSI is designed to reach lower redox potentials in the reduction of the terminal iron sulfur cluster (~−0.5 V) [32] but it achieves this by using a lower redox potential oxidizing terminal in P700 (~+0.45 V) [4]. Once again, nearly half the energy of the photon is consumed in the charge separation. There is enough energy available in the 1.8 eV of the 680–700 nm red photons absorbed by the chlorophylls of PSI and PSII to activate millisecond-long charge separation in an artificial photochemical triad with a donor oxidizing enough to split water into O_2, +1.0 V, in the oxygen-evolving Mn cluster of PSII [3], and an acceptor reducing enough to reduce protons to H_2, −0.42 V at pH 7. Yet natural photosystems are designed to use two red photons to span the H_2O/O_2 and $H+/H_2$ redox gap and they use many more than three redox cofactors to do so. With a basic understanding of the distance scales appropriate for electron tunneling, synthetic chemists and designers of artificial proteins can be expected to step into this design gap.

Acknowledgments This didactic account is the result of the development of engineering for man-made oxidoreductases of the kind proposed in Office of Basic Energy Sciences, Division of Materials Sciences and Engineering [DE-FG02-05ER46223], and the US National Institutes of Health, General Medical Institutes [RO1 GM 41048]. The support from each is nearly equal.

References

1. Byrdin M, Lukacs A, Thiagarajan V, Eker APM, Brettel K, Vos MH. Quantum yield measurements of short-lived photoactivation intermediates in DNA photolyase: toward a detailed understanding of the triple tryptophan electron transfer chain. J Phys Chem A. 2010;114 (9):3207–14.
2. Zeugner A, Byrdin M, Bouly JP, Bakrim N, Giovani B, Brettel K, et al. Light-induced electron transfer in Arabidopsis cryptochrome-1 correlates with in vivo function. J Biol Chem. 2005;280(20):19437–40.
3. Rappaport F, Guergova-Kuras M, Nixon PJ, Diner BA, Lavergne J. Kinetics and pathways of charge recombination in photosystem II. Biochemistry. 2002;41(26):8518–27.
4. Krabben L, Schlodder E, Jordan R, Carbonera D, Giacometti G, Lee H, et al. Influence of the axial ligands on the spectral properties of P700 of photosystem I: a study of site-directed mutants. Biochemistry. 2000;39(42):13012–25.

5. Jordan P, Fromme P, Witt HT, Klukas O, Saenger W, Krauss N. Three-dimensional structure of cyanobacterial photosystem I at 2.5 angstrom resolution. Nature. 2001;411(6840):909–17.
6. Ferreira KN, Iverson TM, Maghlaoui K, Barber J, Iwata S. Architecture of the photosynthetic oxygen-evolving center. Science. 2004;303(5665):1831–8.
7. Deisenhofer J, Epp O, Sinning H, Michel H. Crystallographic refinement at 2.3 Å resolution and refined model of the photosynthetic reaction centre from rhodopseudomonas viridis. J Mol Biol. 1995;246:429–57.
8. Kee HL, Kirmaier C, Tang Q, Diers JR, Muthiah C, Taniguch M, et al. Effects of substituents on synthetic analogs of chlorophylls. Part 1: synthesis, vibrational properties and excited-state decay characteristics. Photochem Photobiol. 2007;83(5):1110–24.
9. Rutherford AW, Osyczka A, Rappaport F. Back-reactions, short-circuits, leaks and other energy wasteful reactions in biological electron transfer: Redox tuning to survive life in O-2. FEBS Lett. 2012;586(5):603–16.
10. Gorman AA, Rodgers MAJ. Current perspectives of singlet oxygen detection in biological environments. J Photochem Photobiol B. 1992;14(3):159–76.
11. Sies H, Menck CFM. Singlet oxygen induced DNA damage. Mutat Res. 1992;275(3–6):367–75.
12. Trebst A, Depka B, Hollander-Czytko H. A specific role for tocopherol and of chemical singlet oxygen quenchers in the maintenance of photosystem II structure and function in Chlamydomonas reinhardtii. FEBS Lett. 2002;516(1–3):156–60.
13. Pross A. The single electron shift as a fundamental process in organic chemistry: the relationship between polar and electron-transfer pathways. Acc Chem Res. 1985;18:212–9.
14. Eberson L. Electron transfer reactions in organic chemistry. New York: Springer-Verlag; 1987. 234 p.
15. Devault D. Quantum-mechanical tunnelling in biological-systems. Q Rev Biophys. 1980;13 (4):387–564.
16. Devault D, Chance B. Studies of photosynthesis using a pulsed laser. I Temperature dependence of cytochrome oxidation rate in Chromatium. Evidence for tunneling. Biophys J. 1966;6 (6):825–47.
17. Moser CC, Keske JM, Warncke K, Farid RS, Dutton PL. Nature of biological electron-transfer. Nature. 1992;355(6363):796–802.
18. Eyring H. The activated complex in chemical reactions. J Chem Phys. 1935;3:107–15.
19. Zwolinski BJ, Marcus RJ, Eyring H. Inorganic oxidation-reduction reactions in solution-electron transfers. Chem Rev. 1955;55(1):157–80.
20. Moser CC, Anderson JLR, Dutton PL. Guidelines for tunneling in enzymes. Biochim Biophys Acta. 2010;1797(8):1573–86.
21. Marcus RA. On the theory of oxidation-reduction reactions involving electron transfer: I. J Chem Phys. 1956;24:966–78.
22. Gunner MR, Dutton PL. Temperature and -delta-G-degrees dependence of the electron-transfer from Bph.- to Qa in Reaction center protein from rhodobacter-sphaeroides with different quinones as Qa. J Am Chem Soc. 1989;111(9):3400–12.
23. Iwaki M, Kumazaki S, Yoshihara K, Erabi T, Itoh S. Delta G(0) dependence of the electron transfer rate in the photosynthetic reaction center of plant photosystem I: Natural optimization of reaction between chlorophyll a (A(0)) and quinone. J Phys Chem. 1996;100(25):10802–9.
24. Lin X, Williams JC, Allen JP, Mathis P. Relationship between rate and free-energy difference for electron-transfer from cytochrome C(2) to the reaction-center in rhodobacter-sphaeroides. Biochemistry. 1994;33(46):13517–23.
25. Woodbury NW, Parson WW, Gunner MR, Prince RC, Dutton PL. Radical-pair energetics and decay mechanisms in reaction centers containing anthraquinones, naphthoquinones or benzoquinones in place of ubiquinone. Biochim Biophys Acta. 1986;851(1):6–22.
26. Lin X, Murchison HA, Nagarajan V, Parson WW, Allen JP, Williams JC. Specific alteration of the oxidation potential of the electron-donor in reaction centers from rhodobacter-sphaeroides. Proc Natl Acad Sci U S A. 1994;91(22):10265–9.

27. Hopfield JJ. Electron transfer between biological molecules by thermally activated tunneling. Proc Natl Acad Sci U S A. 1974;71:3640–4.
28. Jortner J. Temperature-dependent activation-energy for electron-transfer between biological molecules. J Chem Phys. 1976;64(12):4860–7.
29. Crofts AR, Rose S. Marcus treatment of endergonic reactions: a commentary. Biochim Biophy Acta. 2007;1767(10):1228–32.
30. Moser CC, Chobot SE, Page CC, Dutton PL. Distance metrics for heme protein electron tunneling. Biochim Biophy Acta. 2008;1777(7–8):1032–7.
31. Page CC, Moser CC, Chen XX, Dutton PL. Natural engineering principles of electron tunnelling in biological oxidation-reduction. Nature. 1999;402(6757):47–52.
32. Evans MCW, Heathcote P. Effects of glycerol on the redox properties of the electron-acceptor complex in spinach photosystem-I particles. Biochim Biophy Acta. 1980;590(1):89–96.